*Int. J. Electrochem. Sci.*, 17 **(2022)** Article Number: 220232, doi: 10.20964/2022.02.33

International Journal of
ELECTROCHEMICAL
SCIENCE
www.electrochemsci.org

# Preparation of Electrochemical Sensor Based on Magnetic Graphene Nanocomposite for Determination of Dopamine

*Weiwei Wang*[*], *Fan Wei, Baiping Han*

School of Physics and New Energy, Xuzhou University of Technology, Xuzhou, Jiangsu 221018, People's Republic of China
[*]E-mail: wwwang@xzit.edu.cn, weifanqi@mail.ustc.edu.cn, baiping09290@163.com

*Received:* 7 November 2021 / *Accepted:* 7 December 2021 / *Published:* 5 January 2022

This work was focused on the preparation of an electrochemical sensor based on magnetic graphene nanocomposite for the determination of dopamine (DA) in human plasma samples. The electrodeposition method was used for the synthesis of magnetic graphene nanocomposite based on Fe–Ni bimetal oxides ($Fe_2O_3$-NiO) and graphene oxide (GO) on a glassy carbon electrode (GCE). $Fe_2O_3$-NiO@GO/GCE using XRD and SEM confirmed the simultaneous electrodeposition of Fe–Ni bimetal oxide nanoparticles in the spherical-shaped 2D wrinkled stack of ultra-thin GO nanosheets without any aggregation. Electrochemical analyses using DPV and amperometry techniques showed the good electrocatalytic activity, stability, and selectivity of $Fe_2O_3$-NiO@GO/GCE towards the oxidation of DA with rapid electron transfer and mass transport. Furthermore, the sensitivity and detection limit of magnetic graphene nanocomposite sensors were obtained at 0.16812μA/μM and 0.005μM, respectively, which were compared with the other reported DA electrochemical sensors and the results indicated comparable detection limit values and broader linear range of $Fe_2O_3$-NiO@GO/GCE for the determination of DA. The practical capability of $Fe_2O_3$-NiO@GO/GCE for the determination of DA was investigated in prepared real samples of human blood serum of six patients aged 55 to 70 years who were administered an intropin injection. Results showed that there was good agreement between the amperometry and ELISA measurements, and the obtained RSD ranged from 3.08% to 4.36% illustrated the acceptable accuracy of both techniques, especially $Fe_2O_3$-NiO@GO/GCE as a reliable and accurate electrochemical DA sensor in clinical and pharmaceutical analyses.

**Keywords:** Dopamine; Magnetic graphene nanocomposite; Fe–Ni bimetal oxides; Graphene oxide; Amperometry

## 1. INTRODUCTION

Dopamine (DA, 4-(2-Aminoethyl) pyrocatechol), as the third endogenous catecholamine, is a hormone and it is free from the hypothalamus. In the human body, DA is a neurotransmitter that the

nervous system uses to deliver signals between nerve cells [1, 2]. It's found in both central and peripheral nervous system neurons, where it interacts to certain membrane receptors and is stored in vesicles at axon terminals. It released when the neuron is depolarized. DA binds to receptors that are particular for it and have signaling qualities that are similar [3, 4]. They do, however, have separate signaling routes. All DA receptors are G protein-coupled receptors, meaning that their signaling is predominantly mediated by G protein contact and activation [5]. They're also known as serpentine receptors because of the way they wind back and forth across the membrane like a snake. DA interacts with specific membrane receptors to produce its effects [6]. As a result, it is critical for controlling emotion, learning, cognition, working memory, and locomotion [7].

Hypotension (low blood pressure), decreased cardiac output, and impaired perfusion of bodily organs caused by shock, trauma, or sepsis are all treated with DA [8, 9]. It has a sympathetic nervous system effect. The use of DA causes an increase in heart rate and blood pressure. It increases blood pressure and cardiac output by acting through the sympathetic nervous system to raise heart rate and heart muscle contraction force at low doses. Higher doses produce vasoconstriction, which raises blood pressure even further [10]. Because DA cannot cross the blood-brain barrier, it has no effect on the central nervous system when taken as a medication. Some brain illnesses necessitate the use of DA. Dopa-responsive dystonia and Parkinson's disease are examples of such illnesses [11]. Levodopa is prescribed for these patients. It is a DA precursor. It has the ability to pass the blood-brain barrier. However, at the higher doses, side effects of DA include heart arrhythmias, chills, anxiety, shortness of breath, irregular heartbeats that can be gangrene of digits, kidney damage, and life-threatening [12].

Therefore, as well as being an important level of DA in the human body, dosage and timing are also important for the administration of DA [13]. Many studies have been carried out to determine the DA level in clinical and pharmaceutical samples [14]. These have included fluorimetric and spectrophotometric assays [15, 16], liquid chromatography and mass spectrometry analyses [17], and electrochemical techniques [18-21]. Among these methods, electrochemical sensors and biosensors as the device can transform electrochemical and biochemical information, such as analyte concentrations, into analytically signals [22]. These sensors have demonstrated the advantages of great reproducibility, broad linear range, good sensitivity, and low detection limits [23]. Moreover, studies have been shown that modification the electrode surface can enhance the surface-to-volume ratio and promote the performance of electrochemical sensors and biosensors [24, 25]. In addition, many studies have been carried out for the electrochemical determination of DA using modified electrodes with Nobel metals [19, 26-31] which are not affordable, and using modified graphene and CNTs nanocomposites and hybrids [29, 32-46] which show a higher value for detection limit than that in clinical samples or biological fluids such as urine and blood. As a result, more research is needed to develop a more cost-effective composition with a suitable linear range and detection limit values, as well as greater accuracy for clinical applications. Thus, this study was focused on the facile preparation of magnetic graphene nanocomposite as a low-cost electrochemical sensor and application for the determination of DA in human plasma samples.

## 2. EXPERIMENTAL

### *2.1. Preparation of $Fe_2O_3$-NiO@GO/GCE*

The electrochemical deposition technique was used for modification of the GCE with the magnetic GO nanocomposite [47, 48]. For preparation of the electrochemical electrolyte, 100 mg of GO (Xiamen Tob New Energy Technology Co., Ltd., China) nanosheets were dispersed in 100 ml of 0.1 M phosphate buffer solutions (PBS) pH 8.0. The PBS prepared from a mixture of $Na_2HPO_4$ (99%, Xinxiang Huaxing Chemical Co., Ltd., China) and $NaH_2PO_4$ (98%, Shifang Anda Chemicals Co., Ltd., China) in an equal ratio. The dispersed GO was exfoliated during the 60 minutes' sonication period. 5mM $FeCl_3$ (97%, Sigma-Aldrich), 5mM $NiCl_2.6H_2O$ (98%, Sigma-Aldrich and 0.1 M $H_2O_2$ (30 % (w/w), Sigma-Aldrich) were added to dispersed suspension GO. Before the modification of GCE, the GCE was repeatedly polished in alumina powder (99.99%, 0.3 and 0.05 μm, Sigma-Aldrich), and sequentially was sonicated in a mixture of deionized water (DI) and ethanol (95%, Shandong Aojin Chemical Technology Co., Ltd., China) for 12 minutes. The electrochemical syntheses and measurements were done using a potentiostat/galvanostat in a compartment three-electrode electrochemical cell which contained an Ag/AgCl/3M KCl as a reference, platinum mesh as the auxiliary electrode and a clean GCE as a working electrode. The prepared electrolyte gently was stirred during the electrodeposition. Potentiodynamic electrodeposition of nanocomposite of GO and $Fe_2O_3$ was performed using the CV technique at a potential between -1.5 and 0.5 V at 50 mV/s scanning rate for 30 cycles.

### *2.2. Preparation of actual samples*

Blood serum samples of six patients aged 55 to 70 years were provided who administered an intropin injection (contain 40mg/ml DA) in the Heart Disease Diagnosis and Treatment Center, Beijing Chuiyangliu Hospital (Beijing, China). The blood serum samples were provided after five hours of administration. The samples were centrifuged at 2500 rpm for 15 minutes. The obtained supernatants were transferred to an electrochemical cell and used to prepare 0.1 M PBS pH 7.5. These were utilized as real samples. The amperometric analyses were carried out using $Fe_2O_3$-NiO@GO/GCE for the determination of the DA content in prepared real samples at 0.20 V. The DA ELISA Kits (SLC6A3/Dopamine Transporter, detection range: 0.16 - 10 ng/ml, Colorimetric - 450nm (TMB), Lifespan Biosciences, Washington, USA) were also used for the determination of the DA level in blood serum samples.

### *2.3. Electrochemical and structural characterizations*

Differential pulse voltammetry (DPV) and amperometry measurements were performed using an Autolab potentiostat/galvanostat in 0.1 M PBS pH 7.5. The morphological and structural properties of electrodeposited nanostructures were characterized using scanning electron microscopy (SEM) and X-ray diffraction (XRD) at 1.5404 Å (Cu Kα).

## 3. RESULTS AND DISCUSSION

Figure 1 shows the surface morphologies of GO/GCE and $Fe_2O_3$-NiO@GO/GCE. The SEM image of GO/GCE in Figure 1a shows a highly rippled, crumpled and wrinkled stack of ultra-thin GO nanosheets with a porous structure on the GCE surface. Figure 2b shows that in Fe–Ni bimetal oxides, spherical nanoparticles are decorated homogenously on 2D nanosheets of GO without aggregation, indicating a high porosity and large electroactive surface for analyte ion diffusion and the ability to accelerate the redox reaction [49-51].

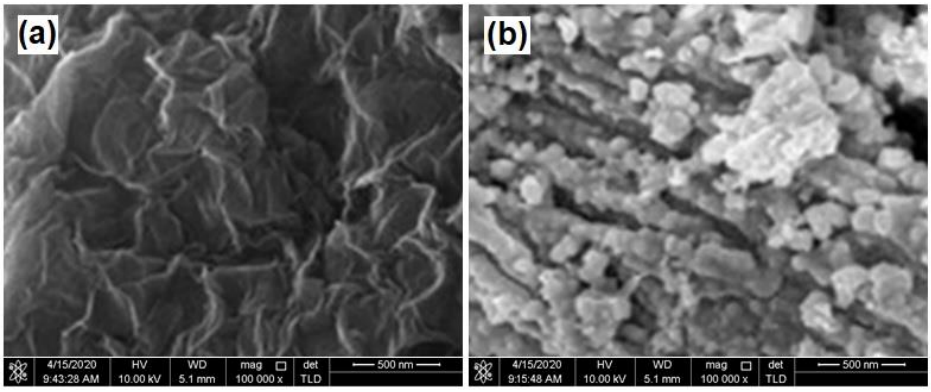


**Figure 1.** SEM image of surface of (a) GO/GCE (b) $Fe_2O_3$-NiO@GO/GCE

XRD patterns of surface of powder of synthesized GO, $Fe_2O_3$@GO, NiO@GO and $Fe_2O_3$-NiO@GO on the GCE surface are presented in Figure 2.

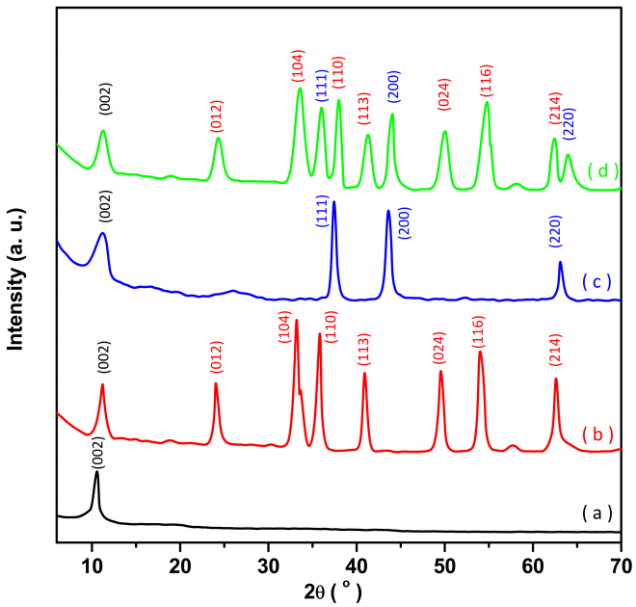


**Figure 2.** XRD pattern of synthesized (a) GO, (b) $Fe_2O_3$/GO, (c) NiO@GO and (d) $Fe_2O_3$-NiO@GO.

As seen from Figure 2a, there is a strong peak at 10.68° in the crystalline structures of GO that is related to the (001) plane of GO [52]. The XRD patterns of $Fe_2O_3$@GO nanocomposites show the (001) plane of GO and the main diffraction peaks at 24.06°, 33.21°, 35.71°, 40.98°, 49.61°, 54.01° and 62.52° that are assigned to the rhombohedral structure of $Fe_2O_3$ with planes of (012), (104), (110), (113),(024), (116) and (214), respectively (JCPDS card no. 04-015-9569). The XRD patterns of NiO@GO nanocomposites in Figure 2c depict the (001) plane of GO and the (111), (200) and (220) planes of the diffraction peaks at 37.34°, 43.06°, and 63.15° that are attributed to the fcc phase of NiO, respectively (JCPDS card no. 00-04–0850). The XRD patterns of $Fe_2O_3$-NiO@GO nanocomposites in Figure 2d simultaneously shows the diffraction peaks of $Fe_2O_3$, NiO and GO, which confirms the simultaneous electrodeposition of GO nanosheets, NiO and $Fe_2O_3$ nanoparticles on the GCE surface.

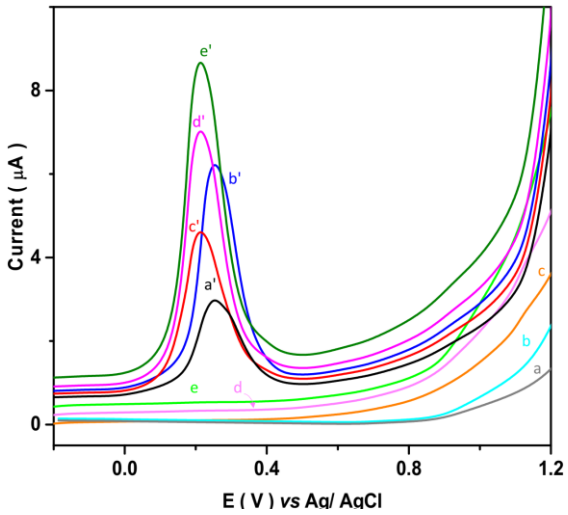


**Figure 3.** DPV curves of (a and a') GCE, (b and b') GO/GCE, (c and c') $Fe_2O_3$/GCE, (d and d') $Fe_2O_3$@GO/GCE and (e and e') $Fe_2O_3$-NiO@GO/GCE in 0.1M PBS pH7.5 in potential range from -1.25 to 0.2V at 10 mV/s scanning rate in absence and presence of 50 µM DA.

Figure 3 exhibits the DPV curves of GCE, $Fe_2O_3$/GCE, GO/GCE, $Fe_2O_3$@GO/GCE and $Fe_2O_3$-NiO@GO/GCE in 0.1M PBS pH7.5 in the potential range from -1.25 to 0.2V at 10mV/s scanning rate in the absence and presence of 50 µM DA. It can be observed, the DPV curves of all electrodes don't show any redox peak in absence of DA. After addition of 50 µM DA, the obvious anodic peaks were observed at 0.26V, 0.20V, 0.25V, 0.20V and 0.20V for GCE, $Fe_2O_3$/GCE, GO/GCE, $Fe_2O_3$@GO/GCE and $Fe_2O_3$-NiO@GO/GCE, respectively which were attributed to the oxidation of o-diphenol groups of DA to reactive o-quinones [53]. Comparison between peak current of GCE, $Fe_2O_3$/GCE, GO/GCE and $Fe_2O_3$@GO/GCE indicates to the GO role to enhance the electrocatalytic current due to electrical conductivity, high surface area and magnificent porosity [54, 55]. Moreover, $Fe_2O_3$ nanoparticles shift the oxidation potential towards a low positive potential because $Fe_2O_3$ nanoparticles can act as an electron transfer mediator and promote electron transfer in the electrochemical oxidation of DA. The introduction of $Fe_2O_3$ nanoparticle onto the GO nanosheets facilitates the conduction pathway at the modified electrode [20]. It is observed that the higher peak current belongs to $Fe_2O_3$-NiO@GO/GCE that is related to the good electrocatalytic activity of Ni towards the oxidation DA with rapid electron

transfer and mass transport [56, 57]. Moreover, the porous morphology of $Fe_2O_3$-NiO@GO/GCE effects on redox behaviors [58].

Further electrochemical studies were conducted on the amperometry technique. Figure 4 displays the amperometric measurements of GCE, $Fe_2O_3$/GCE, GO/GCE, $Fe_2O_3$@GO/GCE and $Fe_2O_3$-NiO@GO/GCE in 0.1M PBS pH7.5 at potentials of 0.26V, 0.20V, 0.25V, 0.20V and 0.20V, respectively. As seen, after the addition of the 100 µM DA solution in 120s, the amperometric currents of all electrodes is increased. In addition, the amperometric responses of the GCE, $Fe_2O_3$/GCE, GO/GCE, $Fe_2O_3$@GO/GCE and $Fe_2O_3$-NiO@GO/GCE after 380s of addition the 100 µM DA solution in the electrochemical cell reveal a 27%, 18%, 20%, 15% and 8% decrease in electrocatalytic current, demonstrating to stable response of $Fe_2O_3$-NiO@GO/GCE to determination of DA because the flexible properties, good adhesion, excellent electronic and mechanical properties of the GO which can enhance the electrocatalytic performance of $Fe_2O_3$-NiO-based catalyst. The abundant functional groups on the surface of GO nanosheets are also favorable for interacting more strongly with magnetic particles and tuning the morphology of electrocatalysts [59, 60]. The interface between Fe–Ni bimetal oxides and GO nanosheets can also stabilize active surface catalytic sites and enable their synergetic effects [61]. Therefore, the following amperometric studies to investigate the sensitivity, detection limit, linear range, selectivity and accuracy of DA sensing were performed using $Fe_2O_3$-NiO@GO/GCE.

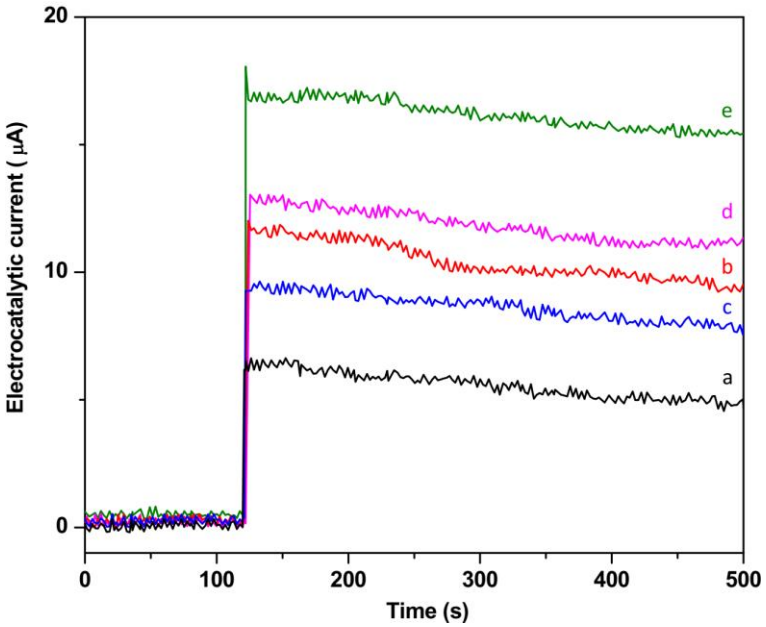


**Figure 4**. Amperometric responses of (e) GCE, (d) GO/GCE, (c) $Fe_2O_3$/GCE, (b) $Fe_2O_3$@GO/GCE and (e) $Fe_2O_3$-NiO@GO/GCE to addition 100µM DA in 0.1M PBS pH7.5 at potential of 0.26V, 0.20V, 0.25V, 0.20V and 0.20V, respectively

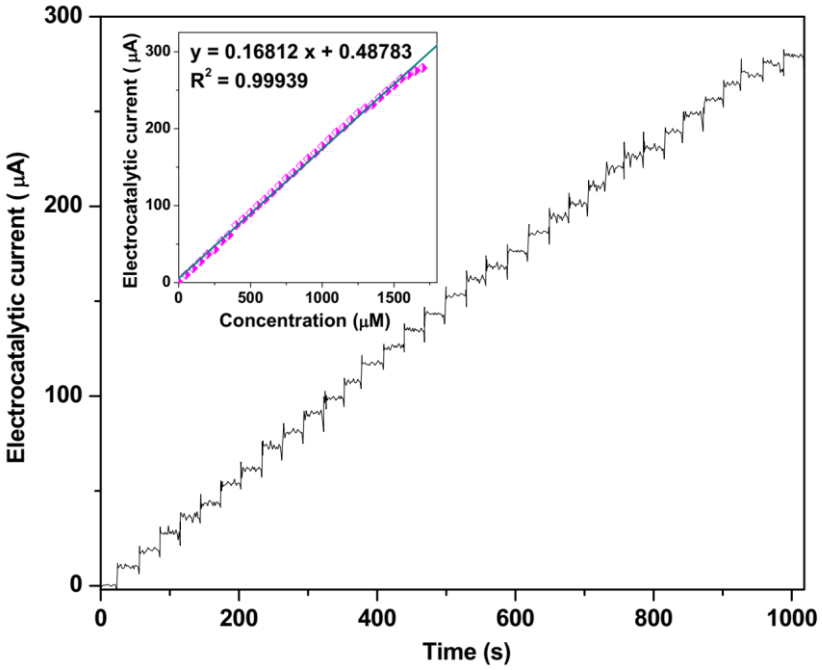


**Figure 5.** Amperometric responses and calibration plot of $Fe_2O_3$-NiO@GO/GCE to successive addition 50μM DA in 0.1M PBS pH7.5 at 0.20V.

Figure 5 depicts the amperometric responses and calibration plot of $Fe_2O_3$-NiO@GO/GCE to successive addition of 50μM DA in 0.1M PBS pH7.5 at 0.20V. It is illustrated by the very fast responses of the proposed electrode to successive additions of DA. Furthermore, the obtained linear range is between 10 and 1500 μM. The obtained sensitivity is 0.16812μA/μM with a detection limit of 0.005 μM which is compared with the other reported DA electrochemical sensors in Table 1. The results from Table 1 indicates that the comparable detection limit values and broader linear range of $Fe_2O_3$-NiO@GO/GCE to determination DA that are associated with the great catalytic capability of the carbon nanostructures and magnetic nanoparticles due to the synergistic effect between GO and Fe–Ni bimetal oxides in magnetic nanocomposite [62].

Table 2 shows the results of the interference effect on DA determination using $Fe_2O_3$-NiO@GO/GCE through the amperometry method in 0.1M PBS pH7.5 at 0.20V with the addition of 10μM of DA and 50μM of some metabolic species in body fluids and drugs that are co-administered with DA. Ascorbic acid, uric acid and serotonin are the most common substance that it shows the interference capability on DA determination [18-21]. As observed from Table 2, the electrochatalytic response of $Fe_2O_3$-NiO@GO/GCE to the addition of 10μM of DA is significantly greater than that to the addition of 50μM of interfering agents. The weak response of the proposed sensor to interfering agents indicates that these interfering species don't show any observable interference effect on DA detection.

**Table 1.** Comparing between the sensing properties of $Fe_2O_3$-NiO@GO/GCE and other reported DA electrochemical sensors.

| **Electrodes** | **Technique** | **Linear range (µM)** | **Detection Limit (µM)** | **Ref.** |
|---|---|---|---|---|
| $Fe_2O_3$-NiO@GO/GCE | Amperometry | 10-1500 | 0.005 | This work |
| $RuS_2$ nanoparticles | Amperometry | 10–80 | 73.8 | [26] |
| Ceramic–graphite composite | Amperometry | 6.6–1200 | 1.4 | [33] |
| Graphene modified electrode | CV | 2.5-100 | 0.5 | [32] |
| Carbon-doped hexagonal boron nitrogen | CV | 40–300 | 0.0058 | [35] |
| GCE | CV | 12– 80 | 0.03 | [34] |
| $NH_2$-$Fe_3O_4$@ graphene sheets | DPV | 0.2-38 | 0.126 | [36] |
| rGO | DPV | 0.5-60 | 0.5 | [37] |
| Flower shaped ZnO | DPV | 0.1 -16 | 0.04 | [38] |
| Pt NPs/rGO | DPV | 10-170 | 0.25 | [19] |
| Holey nitrogen-doped graphene aerogel | DPV | 0.6–75 | 0.22 | [21] |
| poly(o-phenylenediamine)/rGO | DPV | 10-800 | 7.5 | [39] |
| Nitrogen doped graphene | DPV | 0.5-170 | 0.25 | [40] |
| $TiO_2$ nanoparticles/GCE | DPV | 0.08–20 | 0.031 | [41] |
| Exfoliated flexible graphite paper | DPV | 0.5-35 | 0.01 | [42] |
| polypyrrole/rGO core–shell | DPV | 0.06-8 | 0.006 | [43] |
| Au nanoparticles/β-cyclodextrin/Graphene | DPV | 0.5-150 | 0.15 | [28] |
| Graphene nanosheets/Carbon paste electrode | DPV | 2-1000 | 0.85 | [44] |
| Ionic liquid functionalized graphene/GCE | DPV | 5-275 | 0.812 | [45] |
| AuNPs/ tryptophan-functionalized graphene | DPV | 0.5–411 | 0.05 | [27] |
| Graphene flowers/Carbon fiber | DPV | 0.7-45.21 | 0.5 | [46] |
| Pd nanoparticles /graphene/chitosan/GCE | DPV | 0.5-200 | 0.1 | [30] |
| Ag−Pt/nanoporous carbon nanofibers | DPV | 10−500 | 0.11 | [31] |
| Overoxidized polyimidazole/GO | DPV | 12-278 | 0.63 | [29] |
| MWNTs-$SiO_2$-chitosan composites/screen-printed electrode | SWV | 1-20 | 0.2 | [18] |

SWV: Square wave voltammetry

**Table 2.** Results of the interference effect on DA determination using $Fe_2O_3$-NiO@GO/GCE through the amperometry method in 0.1M PBS pH7.5 at 0.20V and addition 10µM of DA and 50µM of interfering agents.

| **Substances** | **Added(µM)** | **Amperometric current response(µA)** | **RSD(%)** |
|---|---|---|---|
| Dopamine | 10 | 1.6832 | ±0.0332 |
| Ascorbic acid | 50 | 0.3711 | ±0.0100 |
| Uric acid | 50 | 0.4090 | ±0.0080 |
| Serotonin | 50 | 0.2290 | ±0.0077 |
| Saccharose | 50 | 0.0920 | ±0.0068 |
| Glucose | 50 | 0.0781 | ±0.0037 |
| Carbidopa | 50 | 0.1190 | ±0.0028 |
| Donepezil | 50 | 0.1108 | ±0.0021 |
| Levodopa | 50 | 0.2005 | ±0.0028 |
| Apomorphine | 50 | 0.0938 | ±0.0018 |
| Ropinirole | 50 | 0.0829 | ±0.0010 |
| Urea | 50 | 0.0169 | ±0.0011 |
| $NH_4^+$ | 50 | 0.0219 | ±0.0011 |
| $NO_3^-$ | 50 | 0.0715 | ±0.0007 |
| $Ca^{2+}$ | 50 | 0.0210 | ±0.0009 |
| $Al^{3+}$ | 50 | 0.0280 | ±0.0013 |
| $Mg^{2+}$ | 50 | 0.0769 | ±0.0017 |
| $Cu^{2+}$ | 50 | 0.0833 | ±0.0018 |
| $Fe^{2+}$ | 50 | 0.0778 | ±0.0014 |
| $K^+$ | 50 | 0.0939 | ±0.0013 |

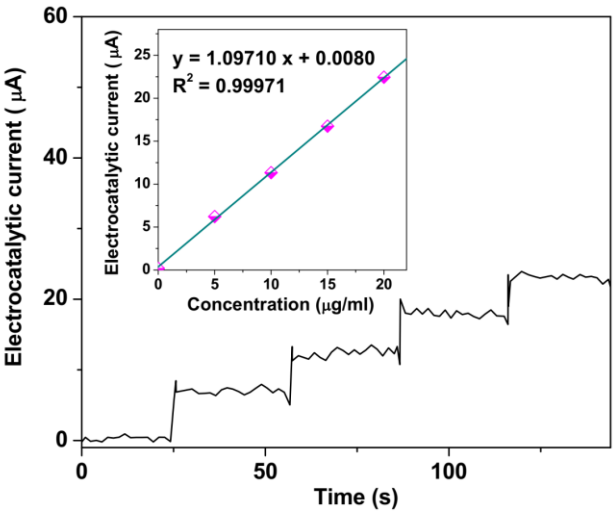


**Figure 6.** Amperometric responses and calibration plot of $Fe_2O_3$-NiO@GO/GCE to successive addition 5µg/ml DA in prepared 0.1M PBS pH7.5 of blood serum at 0.20V.

The practical capability of $Fe_2O_3$-NiO@GO/GCE for the determination of DA in human blood serum is being investigated. The blood serum of six patients aged 55 to 70 years who received an intropin injection. Figure 6 shows the amperometric response and attained calibration plot of $Fe_2O_3$-NiO@GO/GCE to successive addition of 5µg/ml DA solution. As seen from Figure 6 and Table 3, the DA content in the prepared specimen of first patient is 7.29 ng/ml ($7.29\times10^{-3}$ µg/ml), which is near to the obtained results by DA ELISA kit. These measurements were repeated on the other 5 patients, and the results of an average of 5 determinations of DA for each sample are presented in Table 3. As observed, there is good agreement between the amperometry and ELISA measurements, and the obtained RSD range from 3.08% to 4.36% illustrates the acceptable accuracy of both of techniques, especially $Fe_2O_3$-NiO@GO/GCE as reliable and accurate electrochemical DA sensor in clinical and pharmaceutical analyses.

**Table 3.** Results of determinations of DA content in prepared samples of blood serum of six patients aged 55 to 70 years who administered intropin injection using amperometry and ELISA techniques.

| **Sample No.** | **PNS level in prepared samples of blood serum (ng/ml)** | | | |
|---|---|---|---|---|
| | **Amperometry** | | **ELISA** | |
| | $Fe_2O_3$-NiO@GO/GCE | **RSD (%)** | **ELISA** | **RSD (%)** |
| 1 | 7.29 | ±3.22 | 7.98 | ±3.33 |
| 2 | 8.01 | ±4.21 | 8.10 | ±4.32 |
| 3 | 7.94 | ±4.11 | 8.05 | ±3.97 |
| 4 | 8.12 | ±4.08 | 8.17 | ±3.88 |
| 5 | 8.24 | ±3.22 | 8.20 | ±3.73 |
| 6 | 7.99 | ±3.08 | 8.02 | ±4.36 |

## 4. CONCLUSIONS

This work presented the preparation of the electrochemical sensor based on $Fe_2O_3$-NiO@GO nanocomposite as **a** magnetic graphene nanocomposite for the detection of DA in human plasma samples. The electrodeposition method was used for the preparation of $Fe_2O_3$-NiO@GO on GCE. Results of structural and morphological characterizations of $Fe_2O_3$-NiO@GO/GCE confirmed the simultaneous electrodeposition of Fe–Ni bimetal oxide nanoparticles in the spherical-shaped 2D wrinkled stack of ultra-thin GO nanosheets without any aggregation. Results of electrochemical analyses showed to good stability and selectivity of $Fe_2O_3$-NiO@GO/GCE towards the oxidation DA with a linear range of 10 to 1500 µM, detection limit of 0.005 µM and sensitivity of 0.16812 µA/µM which were compared with the other reported DA electrochemical sensors and results indicated comparable detection limit values and broader linear range of $Fe_2O_3$-NiO@GO/GCE to determination DA. The results of the study the practical capability of $Fe_2O_3$-NiO@GO/GCE for the determination of DA in prepared real samples of human blood serum of six patients aged 55 to 70 years who were administered an intropin injection showed that there were good agreement between the amperometry

and ELISA measurements, and the obtained acceptable accuracy of both techniques, especially $Fe_2O_3$-NiO@GO/GCE indicated a reliable and accuracy of $Fe_2O_3$-NiO@GO/GCE as an electrochemical DA sensor in clinical and pharmaceutical analyses.

ACKNOWLEDGMENTS
National Natural Science Foundation of China: Statistical properties of single molecule spectrum under pump-probe fields 11247233.

## References

1. S. Basu and P.S. Dasgupta, *Journal of neuroimmunology*, 102 (2000) 113.
2. L. Jia, Y. Yu, Z.-p. Li, S.-n. Qin, J.-r. Guo, Y.-q. Zhang, J.-c. Wang, J.-c. Zhang, B.-g. Fan and Y. Jin, *Bioresource Technology*, 332 (2021) 125086.
3. M.K. Kelm, H.E. Criswell and G.R. Breese, *Brain research reviews*, 65 (2011) 113.
4. H. Karimi-Maleh, Y. Orooji, F. Karimi, M. Alizadeh, M. Baghayeri, J. Rouhi, S. Tajik, H. Beitollahi, S. Agarwal and V.K. Gupta, *Biosensors and Bioelectronics*, 184 (2021) 113252.
5. H. Guan, S. Huang, J. Ding, F. Tian, Q. Xu and J. Zhao, *Acta Materialia*, 187 (2020) 122.
6. X. Tong, F. Zhang, B. Ji, M. Sheng and Y. Tang, *Advanced Materials*, 28 (2016) 9979.
7. M. Wang, C. Jiang, S. Zhang, X. Song, Y. Tang and H.-M. Cheng, *Nature chemistry*, 10 (2018) 667.
8. R.J. Beale, S.M. Hollenberg, J.-L. Vincent and J.E. Parrillo, *Critical care medicine*, 32 (2004) S455.
9. Y. Orooji, B. Tanhaei, A. Ayati, S.H. Tabrizi, M. Alizadeh, F.F. Bamoharram, F. Karimi, S. Salmanpour, J. Rouhi and S. Afshar, *Chemosphere*, 281 (2021) 130795.
10. G. Yang, X. Feng, W. Wang, Q. OuYang and L. Liu, *Composites Science and Technology*, 213 (2021) 108959.
11. C. Eggers, A.E. Volk, D. Kahraman, G.R. Fink, B. Leube, M. Schmidt and L. Timmermann, *Parkinsonism & related disorders*, 18 (2012) 666.
12. X. Zhang, Y. Tang, F. Zhang and C.S. Lee, *Advanced Energy Materials*, 6 (2016) 1502588.
13. R. Wang, C. He, W. Chen, L. Fu, C. Zhao, J. Huo and C. Sun, *Nanoscale*, 13 (2021) 19247.
14. X. Ji, C. Hou, M. Shi, Y. Yan and Y. Liu, *Food Reviews International*, (2020) 1.
15. C. Atack, *British journal of pharmacology*, 48 (1973)
16. M. Mamiński, M. Olejniczak, M. Chudy, A. Dybko and Z. Brzózka, *Analytica chimica acta*, 540 (2005) 153.
17. V. Carrera, E. Sabater, E. Vilanova and M.A. Sogorb, *Journal of Chromatography B*, 847 (2007) 88.
18. S. Wang, Y. Wang, Q. Min, T. Shu, X. Zhu, A. Peng and H. Ding, *International Journal of Electrochemical Science*, 11 (2016) 2360.
19. T.-Q. Xu, Q.-L. Zhang, J.-N. Zheng, Z.-Y. Lv, J. Wei, A.-J. Wang and J.-J. Feng, *Electrochimica Acta*, 115 (2014) 109.
20. S. Sundar and V. Ganesh, *Scientific reports*, 10 (2020) 1.
21. S. Feng, L. Yu, M. Yan, J. Ye, J. Huang and X. Yang, *Talanta*, 224 (2021) 121851.
22. J. Huo, L. Fu, C. Zhao and C. He, *Chinese Chemical Letters*, 32 (2021) 2269.
23. X. Ji, B. Peng, H. Ding, B. Cui, H. Nie and Y. Yan, *Food Reviews International*, (2021) 1.
24. Z. Savari, S. Soltanian, A. Noorbakhsh, A. Salimi, M. Najafi and P. Servati, *Sensors and Actuators B: Chemical*, 176 (2013) 335.
25. X. Li, Q. Yu, X. Chen and Q. Zhang, *Journal of Magnesium and Alloys*, (2021)

26. J. Deepika, R. Sha and S. Badhulika, *Microchimica Acta*, 186 (2019) 480.
27. Q. Lian, A. Luo, Z. An, Z. Li, Y. Guo, D. Zhang, Z. Xue, X. Zhou and X. Lu, *Applied Surface Science*, 349 (2015) 184.
28. X. Tian, C. Cheng, H. Yuan, J. Du, D. Xiao, S. Xie and M.M. Choi, *Talanta*, 93 (2012) 79.
29. X. Liu, L. Zhang, S. Wei, S. Chen, X. Ou and Q. Lu, *Biosensors and Bioelectronics*, 57 (2014) 232.
30. X. Wang, M. Wu, W. Tang, Y. Zhu, L. Wang, Q. Wang, P. He and Y. Fang, *Journal of Electroanalytical Chemistry*, 695 (2013) 10.
31. Y. Huang, Y.-E. Miao, S. Ji, W.W. Tjiu and T. Liu, *ACS applied materials & interfaces*, 6 (2014) 12449.
32. X. Ma, M. Chao and Z. Wang, *Analytical Methods*, 4 (2012) 1687.
33. D. Ravi Shankaran, N. Uehara and T. Kato, *Analytica Chimica Acta*, 478 (2003) 321.
34. D.-Q. Huang, C. Chen, Y.-M. Wu, H. Zhang, L.-Q. Sheng, H.-J. Xu and Z.-D. Liu, *International Journal of Electrochemical Science*, 7 (2012) 5510.
35. H. Ouyang, W. Li and Y. Long, *Electrochimica Acta*, 369 (2021) 137682.
36. D. Wu, Y. Li, Y. Zhang, P. Wang, Q. Wei and B. Du, *Electrochimica Acta*, 116 (2014) 244.
37. L. Yang, D. Liu, J. Huang and T. You, *Sensors and Actuators B: Chemical*, 193 (2014) 166.
38. D. Balram, K.-Y. Lian and N. Sebastian, *International Journal of Electrochemical Science*, 13 (2018) 1542.
39. X. Liu, H. Zhu and X. Yang, *Rsc Advances*, 4 (2014) 3706.
40. Z.-H. Sheng, X.-Q. Zheng, J.-Y. Xu, W.-J. Bao, F.-B. Wang and X.-H. Xia, *Biosensors and Bioelectronics*, 34 (2012) 125.
41. M. Mazloum-Ardakani, H. Rajabi, H. Beitollahi, B.B.F. Mirjalili, A. Akbari and N. Taghavinia, *International Journal of Electrochemical Science*, 5 (2010) 147.
42. W. Cai, T. Lai, H. Du and J. Ye, *Sensors and Actuators B: Chemical*, 193 (2014) 492.
43. T. Qian, S. Wu and J. Shen, *Chemical Communications*, 49 (2013) 4610.
44. M. Bagherzadeh and M. Heydari, *Analyst*, 138 (2013) 6044.
45. C. Wang, P. Xu and K. Zhuo, *Electroanalysis*, 26 (2014) 191.
46. J. Du, R. Yue, F. Ren, Z. Yao, F. Jiang, P. Yang and Y. Du, *Biosensors and bioelectronics*, 53 (2014) 220.
47. F. Cui and X. Zhang, *Journal of Solid State Electrochemistry*, 17 (2013) 167.
48. A. Kormányos, E. Kecsenovity, A. Honarfar, T. Pullerits and C. Janáky, *Advanced functional materials*, 30 (2020) 2002124.
49. B. Kirubasankar, V. Murugadoss and S. Angaiah, *RSC advances*, 7 (2017) 5853.
50. H. Savaloni, E. Khani, R. Savari, F. Chahshouri and F. Placido, *Applied Physics A*, 127 (2021) 1.
51. R. Savari, H. Savaloni, S. Abbasi and F. Placido, *Sensors and Actuators B: Chemical*, 266 (2018) 620.
52. S.K. Abdel-Aal, A. Ionov, R.N. Mozhchil and A.H. Naqvi, *Applied Physics A*, 124 (2018) 365.
53. S. Schindler and T. Bechtold, *Journal of Electroanalytical Chemistry*, 836 (2019) 94.
54. L. Lin, X. Yao and L. Ma, *International Journal of Electrochemical Science*, 15 (2020) 7763.
55. H. Savaloni, R. Savari and S. Abbasi, *Current Applied Physics*, 18 (2018) 869.
56. J. Gao, P. He, T. Yang, L. Zhou, X. Wang, S. Chen, H. Lei, H. Zhang, B. Jia and J. Liu, *Journal of Electroanalytical Chemistry*, 852 (2019) 113516.
57. F. Chahshouri, H. Savaloni, E. Khani and R. Savari, *Journal of Micromechanics and Microengineering*, 30 (2020) 075001.
58. B.T. Hang and T.T. Anh, *Scientific Reports*, 11 (2021) 1.
59. F. Li, X. Jiang, J. Zhao and S. Zhang, *Nano energy*, 16 (2015) 488.
60. H. Savaloni and R. Savari, *Materials Chemistry and Physics*, 214 (2018) 402.
61. Y. Wang, P. Han, X. Lv, L. Zhang and G. Zheng, *Joule*, 2 (2018) 2551.

62. Z. Zhang, L. Lu and Y. Yi, *Materials Testing*, 63 (2021) 92.